Dynamic Simulation of Vehicle Crosswind Sensitivity for Various Rear Slant Angle

S. Mansor, M. R. Rahman
Department of Aeronautical and Automotive Engineering, Universiti Teknologi Malaysia, 81310 Skudai, Johor, Malaysia.

M.A. Passmore
Department of Aeronautical and Automotive Engineering, Loughborough University, LE11 3TU, UK.

Abstract

The purpose of this paper is to study the effect of rear slant angle of a surface vehicle on crosswind sensitivity. The vehicle model used to conduct a dynamic simulation was based on a simple reduced order lateral dynamics of sideslip and yaw rate motion. It is important to know the effect of the aerodynamic forces and moments on driving stability because it is responsible for the excitation and influences the response of the vehicle. In this work, a mathematical model of vehicle lateral motion is developed using a simple reduced order model coupled with aerodynamics model. The intention here is to compare the effect of rear slant angles responses to crosswind and to rank the crosswind sensitivity ratings. For the purpose of comparison, the tyre cornering stiffness and weight distribution are kept constant for all aerodynamic configurations. The aerodynamic loads are defined as the function of the aerodynamic derivatives from the static wind tunnel tests. Result shows a 20^o rear slant angle demonstrates the highest rating of crosswind sensitivity, while zero degree slant exhibits the least.

Keywords: Crosswind sensitivity, aerodynamic derivatives, wind tunnel, simulation.

Nomenclature

A	- model frontal area	m^2
As	- model side area	m^2
cg	- centre of gravity	
Cy_β	- aerodynamic side force derivative	rad^{-1}
Cy_r	- aerodynamic side force damping derivative	rad^{-1}
Cn_β	- aerodynamic yaw moment derivative	rad^{-1}
Cn_r	- aerodynamic yaw damping derivative	rad^{-1}
Cy	- aerodynamic side force coefficient	
Krf	- front wheel cornering stiffness	$N.rad^{-1}$
Krr	- rear wheel cornering stiffness	$N.rad^{-1}$
ℓcp	- distance between *cp* and *cg*	m
ℓwb	- wheel base length	m
ℓf	- distance between front axle to *cg*	m

ℓr	- distance between rear axle to *cg*	m
N_β	- aerodynamic yaw moment stiffness	$Nm.rad^{-1}$
$N_{\beta c}$	- chassis yaw moment stiffness	$Nm.rad^{-1}$
N_a	- aerodynamic yaw moment	Nm
N_r	- aerodynamic yaw moment damping	$Nms.rad^{-1}$
N_{rc}	- chassis yaw moment damping	$Nms.rad^{-1}$
r	- yaw rate	$rad\ s^{-1}$
$r_{\max}$	- maximum yaw rate	$rad\ s^{-1}$
$r_{(t=1s)}$	- yaw rate after 1 second	$rad\ s^{-1}$
u, v, w	- forward, lateral and vertical speed	$m.s^{-1}$
V	- wind tunnel velocity	$m.s^{-1}$
V_w	- crosswind velocity	$m.s^{-1}$
Y_β	- aerodynamic side force stiffness	$N.rad^{-1}$
$Y_{\beta c}$	- chassis side force stiffness	$N.rad^{-1}$
Y_r	- aerodynamic side force damping	$Ns.rad^{-1}$
Y_{rc}	- chassis side force damping	$Ns.rad^{-1}$
β	- model yaw angle	deg
$\dot{\beta}$	- model yaw velocity	deg/s
$\ddot{\beta}$	- model yaw acceleration	deg/s^2
β_f	- yaw angle fluctuation	deg
β_w	- relative crosswind angle	deg
ρ	- air density	$kg.m^{-3}$
ψ	- crosswind angle with respect to vehicle forward speed	deg

1.0 Introduction

In a real case, for a non-steady motion of a vehicle, the aerodynamic loads influence its overall stiffness and damping characteristics. Prototype vehicles have been used to check vehicle stability by actual driving tests to evaluate the effect of transient aerodynamics, Murgai [1], Hiramatsu and Soma [2]. However at this stage it is often too late to make changes to the vehicle. To reduce the cost of developing a new vehicle and allow early intervention, much research activity has involved developing handling and stability simulations to study the effect of aerodynamics during the design phase, Yip and Crolla [3], Kee et al. [4], Mac Adam [5]. The aerodynamic models used in such simulations are determined from static (steady-state) wind tunnel tests performed on the vehicle, or on a scale model.

2.0 Effect of Rear Slant Angle

Figure 1 shows Davis model with various rear slant angle employed in this paper.

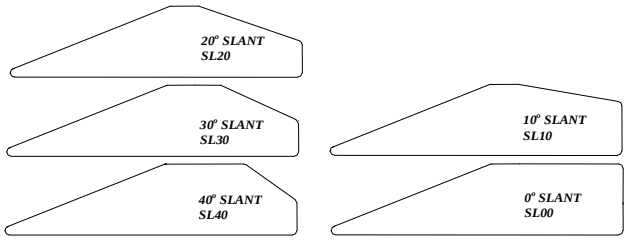

Figure 1 Davis model with various rear slant angle.

In subsequent figures the abbreviation SL20 and etc are used to denote the test configuration. Figure 2 shows the results for varying slant angle from the static (steady state) wind tunnel tests conducted using a 6-component balance to measure side force and yaw moment with yaw angle (sideslip) variations.

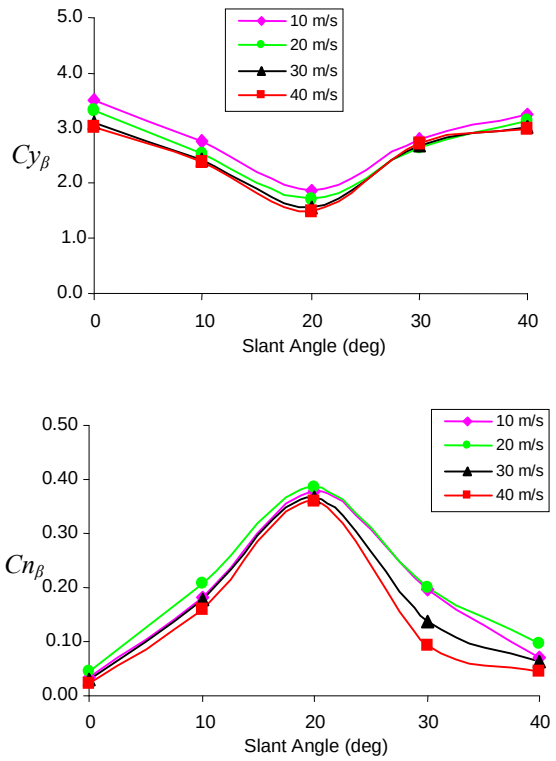

Figure 2 Static aerodynamic side-force and yaw moment derivatives

The results are presented in the form of side-force and yaw moment derivatives for four tunnel speeds between 10 and 40 m/s representing a Reynolds number range of ($4.3x10^5$ to $1.7x10^6$). There is evidently some Reynolds number dependency for all models but this is most pronounced in the yaw moment derivative for the 30° slant angle. As expected the zero and 40 degree slant angles exhibit the highest side-force derivatives and the 20 degree the largest yaw moment derivative.

3.0 Vehicle Lateral Dynamics with Aerodynamic Effect

The dynamic response of a vehicle to wind disturbance is governed by its aerodynamic derivatives coupled with the suspension and tyre characteristics. The equation of motion of a car can be formed by equating the inertial reaction to the external forces. Assuming that the car is moving at a steady forward speed, u without pitching and rolling movements and the results are considered by the yaw rate and sideslip, Milliken [6], Russell [7] and Scibor-Rylsky [8]. Assembling the inertial characteristics and forces in derivative form, then the steering wheel input δ and yaw angle input β is given as follows,

$$\begin{aligned} m(\dot{v}+ur) &= Y_{\beta c}\beta + Y_{rc}r + Y_{\delta c}\delta + Y_A \\ I_{zz}\dot{r} &= N_{\beta c}\beta + N_{rc}r + N_{\delta c}\delta + N_A \end{aligned} \qquad (3.1)$$

where $\dot{v}$ lateral acceleration, r yaw rate and $\dot{r}$ yaw acceleration. The Y_A and N_A is the aerodynamic side force and yaw moment respectively which can expressed as follows,

$$\begin{aligned} Y_A &= Y_\beta(\beta - \beta w) + Y_r r \\ N_A &= N_\beta(\beta - \beta w) + N_r r \end{aligned} \qquad (3.2)$$

Where Y_β, N_β are the dimensional static stability derivatives, while Y_r and N_r are the dimensional dynamic stability derivatives and β_w is the crosswind yaw angle. The dimensional expressions for all the derivatives are given below.

$$\begin{aligned} Y_\beta &= \tfrac{1}{2}\rho u^2 A C_{y\beta} & N_\beta &= \tfrac{1}{2}\rho u^2 A \ell C_{n\beta} \\ Y_r &= \tfrac{1}{2}\rho u A \ell C_{y_r} & N_r &= \tfrac{1}{2}\rho u A \ell^2 C_{n_r} \end{aligned} \qquad (3.3)$$

Substituting Equation (3-2) into Equation (3-1) and rearrange, yields,

$$
\begin{aligned}
m(\dot{v}+ur) &= (Y_{\beta c}+Y_{\beta})\beta + (Y_{rc}+Y_r)r + Y_{\delta c}\delta - Y_{\beta}\beta w \\
I_{zz}\dot{r} &= (N_{\beta c}+N_{\beta})\beta + (N_{rc}+N_r)r + +N_{\delta c}\delta - N_r\beta w
\end{aligned}
\tag{3.4}
$$

The side speed v can be defined as body aerodynamic yaw angle β, for small angle $\beta = \frac{v}{u}$ then $v = u\beta$, for that the derivative of v becomes $\dot{v} = u\dot{\beta} + \dot{u}\beta$. For steady motion, $\dot{u} = 0$, then $\dot{v} = u\dot{\beta}$

$$
\begin{aligned}
mu\dot{\beta} &= (Y_{\beta c}+Y_{\beta})\beta + (Y_{rc}+Y_r - mu)r + Y_{\delta c}\delta - Y_{\beta}\beta w \\
I_{zz}\dot{r} &= (N_{\beta c}+N_{\beta})\beta + (N_{rc}+N_r)r + N_{\delta c}\delta - N_r\beta w
\end{aligned}
\tag{3.5}
$$

The above equation can be simplified to become a reduced order model of yawing motion as follows;

$$
\begin{bmatrix} \dot{\beta} \\ \dot{r} \end{bmatrix} = \begin{bmatrix} \frac{Y_{\beta c}+Y_{\beta}}{mu} & \frac{Y_{rc}+Y_r}{mu} - 1 \\ \frac{N_{\beta c}+N_{\beta}}{I_{zz}} & \frac{N_{rc}+N_r}{I_{zz}} \end{bmatrix} \begin{bmatrix} \beta \\ r \end{bmatrix} + \begin{bmatrix} \frac{Y_{\delta c}}{mu} & -\frac{Y_{\beta}}{mu} \\ \frac{N_{\delta c}}{I_{zz}} & -\frac{N_{\beta}}{mu} \end{bmatrix} \begin{bmatrix} \delta \\ \beta w \end{bmatrix}
\tag{3.6}
$$

The above equation is in the form of state-space equation and can written as, $\dot{x}(t) = Ax(t) + Bu(t)$. The transfer function due to crosswind βw (i.e. $\frac{\beta}{\beta w}$ and $\frac{r}{\beta w}$) can be derived using the expression, $(sI - A)^{-1}.B = \frac{adj|sI - A|}{\det|sI - A|}.B$. For zero steering angle, putting $\delta = 0$, yields

$$
\begin{bmatrix} \frac{\beta}{\beta w} \\ \frac{r}{\beta w} \end{bmatrix} = \begin{bmatrix} s - \frac{Y_{\beta c}+Y_{\beta}}{mu} & \frac{Y_{rc}+Y_r}{mu} + 1 \\ -\frac{N_{\beta c}+N_{\beta}}{I_{zz}} & s - \frac{N_{rc}+N_r}{I_{zz}} \end{bmatrix}^{-1} \begin{bmatrix} -\frac{Y_{\beta}}{mu} \\ -\frac{N_{\beta}}{I_{zz}} \end{bmatrix}
\tag{3.7}
$$

$$
\begin{bmatrix} \frac{\beta}{\beta w} \\ \frac{r}{\beta w} \end{bmatrix} = \frac{\begin{bmatrix} s - \frac{N_{rc}+N_r}{I_{zz}} & \frac{Y_{rc}+Y_r}{mu} - 1 \\ \frac{N_{\beta c}+N_{\beta}}{I_{zz}} & s - \frac{Y_{\beta c}+Y_{\beta}}{mu} \end{bmatrix} \begin{bmatrix} -\frac{Y_{\beta}}{mu} \\ \frac{-N_{\beta}}{I_{zz}} \end{bmatrix}}{\left[s - \frac{N_{rc}+N_r}{I_{zz}} \right] \left[s - \frac{Y_{\beta c}+Y_{\beta}}{mu} \right] - \left[\frac{N_{\beta c}+N_{\beta}}{I_{zz}} \right] \left[\frac{Y_{rc}+Y_r - mu}{mu} \right]}
\tag{3.8}
$$

The system transfer functions are given by:

$$\begin{bmatrix} \frac{\beta}{\beta w} \\ \frac{r}{\beta w} \end{bmatrix} = \frac{\begin{bmatrix} -\frac{Y_\beta}{mu}s + \frac{(N_{rc}+N_r)Y_\beta}{I_{zz}mu} - \frac{(Y_{rc}+Y_r)N_\beta}{muI_{zz}} + \frac{N_\beta}{I_{zz}} \\ -\frac{N_\beta}{I_{zz}}s + \frac{(Y_{\beta c}+Y_\beta)N_\beta}{I_{zz}mu} - \frac{(N_{\beta c}+N_\beta)Y_\beta}{muI_{zz}} \end{bmatrix}}{s^2 - \left[\frac{N_{rc}+N_r}{I_{zz}} + \frac{Y_{\beta c}+Y_\beta}{mu}\right]s - \left[\frac{N_{\beta c}+N_\beta}{I_{zz}}\right]\left[\frac{Y_{rc}+Y_r-mu}{mu}\right] + \left[\left(\frac{N_{rc}+N_r}{I_{zz}}\right)\left(\frac{Y_{\beta c}+Y_\beta}{mu}\right)\right]} \tag{3.9}$$

4.0 Crosswind Angles and Resultant

If the vehicle initially travel at forward speed u with zero yaw angle (i.e. w=0), suddenly experiences a crosswind V_w coming at an angle of ψ with the vehicle forward speed, the resultant relative wind speed V_R can be deduced from the vector diagram from Figure 3

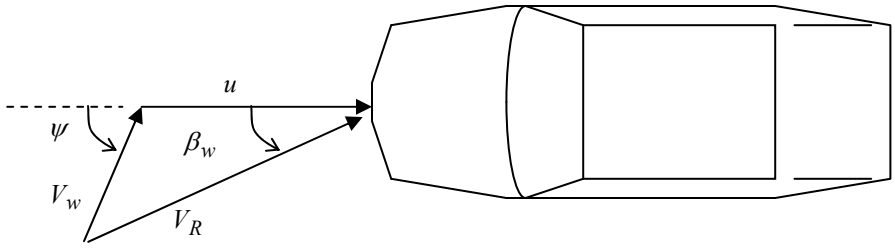

Figure 3 Crosswind angles and resultant.

Where,

u	vehicle speed
V_w	crosswind speed
V_R	relative speed
β_w	relative crosswind angle
ψ	crosswind angle

The equation for relative speed is given by,

$$V_R{}^2 = (u + V_w \cos\psi)^2 + (V_w \sin\psi)^2 = u^2 + 2uV_w \cos\psi + V_w{}^2 \cos^2\psi + V_w{}^2 \sin^2\psi$$

$$V_R = \sqrt{u^2 + 2uV_w \cos\varphi + V_w{}^2} \tag{4.1}$$

The wind yaw angle is given by,

$$\beta_w = \tan^{-1} \frac{V_w \sin\psi}{V_w \cos\psi + u} \tag{4.2}$$

For example if $\psi = 90^o$ (i.e. direction of V_w is perpendicular to vehicle forward speed u), then the resultant speed V_R and the wind yaw angle β_w is given by,

$$V_R = \sqrt{u^2 + {V_w}^2} \tag{4.3}$$

$$\beta_w = \tan^{-1} \frac{V_w}{u} \tag{4.4}$$

5.0 Aerodynamic Derivatives

The aerodynamic derivatives used in the simulation are the side force and yaw moment derivatives measured in the wind tunnel taken at the highest Reynolds number of 1.71×10^6. Table 1 shows the aerodynamic derivatives for all configurations.

Table 1 Aerodynamic side force, yaw moment at Reynolds number 1.71×10^6 for different rear slant angle.

	Aerodynamic Derivatives	
Configurations	$Cy_{\beta_{static}}$ (rad^{-1})	$Cn_{\beta_{static}}$ (rad^{-1})
Rear Slant Angles		
0^o slant (SL00)	3.0309	0.0229
10^o slant (SL10)	2.4064	0.1604
20^o slant (SL20)	1.4954	0.3610
30^o slant (SL30)	2.7273	0.0917
40^o slant (SL40)	2.9794	0.0458

6.0 Simulation Results

The simulation permits the estimation of important parameters such as yaw angle, yaw rate, path deviation and lateral acceleration. The transient parameter of path deviation and yaw rate are compared with different model configurations.

The vehicle baseline data is based on typical value for passenger cars Zhenggi et al. [9]. For the purpose of comparison all models are assumed to have the same chassis parameters as listed in Table 2. For all models the aerodynamic side force and yaw moment derivatives are referenced to mid wheel-base, as measured in the wind tunnel.

Table 2 Vehicle data for simulation [9].

Vehicle weight,	$W = 1200$ kg
Wheel base	$\ell wb = 2.5$ m
Distance between front axle and cg	$\ell f = 1.25$ m
Distance between rear axle and cg	$\ell r = 1.25$ m
Yaw inertia	$I_{zz} = 1600$ kg m^2
Front wheel cornering stiffness	$Krf = -32000$ N/rad
Rear wheel cornering stiffness	$Krr = -41500$ N/rad
Chassis Derivatives:	
Side force stiffness	$Y_{\beta c} = Krf + Krr = -73{,}500$ N/rad
Side force damping	$Y_{rc} = (lfKrf - lrKrr)/u = -430$ Ns/rad
Yaw stiffness	$N_{\beta c} = (lfKrf - lrKrr) = 12051$ Nm/rad
Yaw damping	$N_{rc} = (lf^2 Krf + lr^2 Krr)/u = -4224$ Nms/rad

The vehicle is simulated at 28 m/s forward speed and exposed to a crosswind at the speed of 16 m/s normal to vehicle speed for 1.5 seconds, Goetz [10], Kee et al. [4], Hiramatsu and Soma [2]. The plot of crosswind exposure is shown in Figure 4. The simulation results are shown in Figure 5 for different rear slant angles.

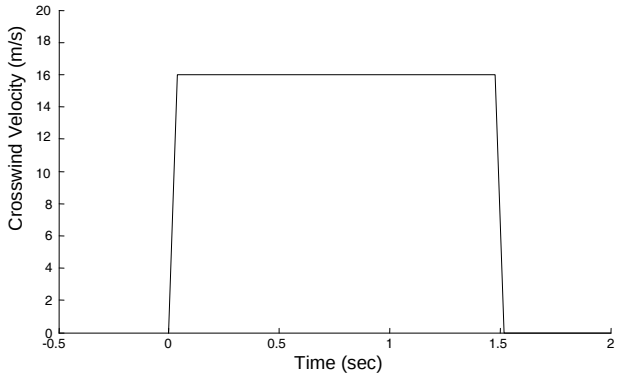

Figure 4 Crosswind input exposure.

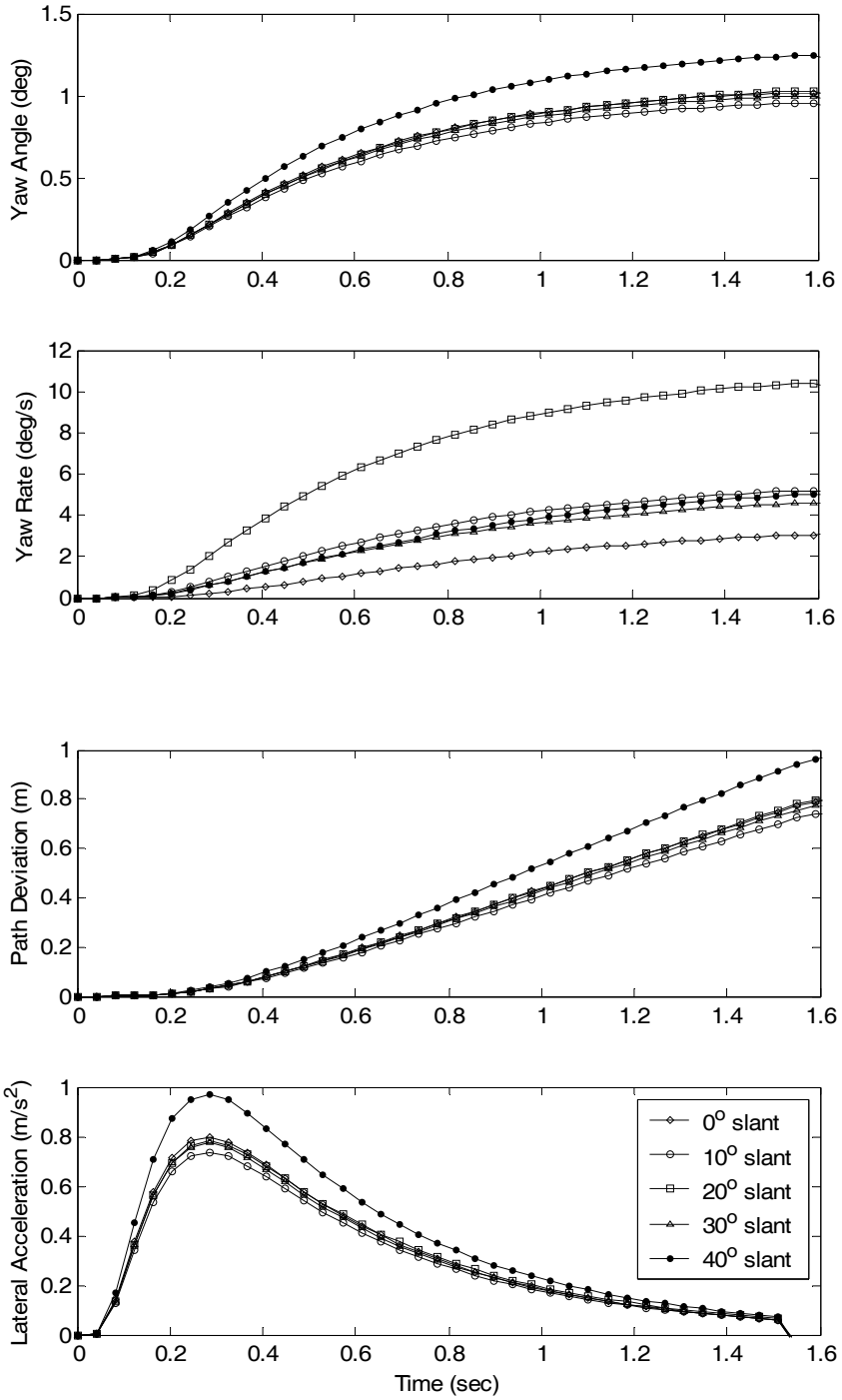

Figure 5 Open loop yaw angle, yaw rate, path deviation and lateral acceleration of different rear slant angles.

Figure 5 shows the effect of rear slant angles on vehicle response. The 20^o slant shows a rapid increase in yaw rate compared to the other models, while zero degree slant shows the least. For all models the maximum value of yaw rate progressively increases with the increase in yaw moment derivative. The maximum value of yaw rate for 20^o slant is more than double the maximum values shown by zero 30^o and 40^o slant angles. It is clearly demonstrated that the increment of yaw rate and the time to reach its maximum value is strongly influenced by the yaw moment derivatives.

For lateral acceleration the 40^o slant shows a rapid increase and has the highest value compared to the others, while the 10^o slant shows the least. The response and peak value of lateral acceleration coincides with the path deviation. The figure shows that the path deviation, lateral acceleration are strongly influenced by the side force derivatives.

It has been predicted that the damping derivatives could influenced the vehicle response to crosswind. However, in all cases, the inclusion of the aerodynamic damping derivatives Cy_r and Cn_r in the simulation has no effect on yaw rate and path deviation. It is concluded that the aerodynamic damping is very small compared to the mechanical damping from the vehicle chassis and therefore does not affect the yaw rate and path deviation.

7.0 Crosswind Sensitivity Rating

In the evaluation of vehicle response to crosswind the important parameters are the path deviation and yaw rate, Howell [11], [12], Murgai [1], Hiramatsu and Soma [2], Milliken [6]. Goetz [10] at Volkswagen developed a rating method in an effort to provide summary information from measured responses for vehicles tested using their crosswind facility. The method relies only on the yaw rate response and is given as S_A:

$$S_A = r_{\max} * t_{(r_{\max})} * r_{(t=1s)} \qquad (7.1)$$

where, $r_{\max}$ = maximum yaw rate

$t_{(r_{\max})}$ = time of maximum yaw rate

$r_{(t=1s)}$ = yaw rate after 1 sec

The formula can be modified to change the dimension of S_A in deg^2/s to deg.

$$S_B = \sqrt{r_{\max} * t_{(r_{\max})} * r_{(t=1s)} * 1s} \qquad (7.2)$$

In the test reported the rating parameter is shown to correlate well with subjective assessments of the same vehicles. A higher sensitivity factor indicates that the car is sensitive to crosswind. The results of the crosswind sensitivity rating for various slant angles using the static aerodynamic derivatives from the simulation are tabulated in Table 3.

Table 3 Open Loop Crosswind sensitivity ratings based on static measured derivatives of different slant angles.

	0^o slant SL00	10^o slant SL10	20^o slant SL20	30^o slant SL30	40^o slant SL40
Maximum yaw rate (deg/sec)	3.19	4.86	7.39	2.91	3.51
Time at maximum yaw rate (sec)	1.63	1.59	1.55	1.59	1.63
Yaw rate after 1 sec (deg/sec)	2.31	3.98	6.46	2.37	2.62
S_B (deg)	3.47	5.55	8.60	3.32	3.87

For all configurations the ratings of the crosswind sensitivity show that yaw moment derivative strongly influences the crosswind sensitivity factor. A 20^o slant demonstrates the highest rating of crosswind sensitivity, while zero degree slant exhibits the least.

8.0 Conclusion

The aerodynamic derivatives show the actual sensitivity of the model. In the simple vehicle simulation the crosswind sensitivity is determined from yaw rate response. The model with large value of positive yaw moment derivative Cn_β generates high yaw rate thus exhibits higher degree of crosswind sensitivity. The side force derivative Cy_β has strong effects on path deviation. Using a simple bluff body vehicle shape a 20^o slant

demonstrates the highest rating of crosswind sensitivity, while zero degree slant exhibits the least.

References

[1] Murgai N, "*Effect of Cross Winds on Road and Rail Vehicles*", Aerospace Engineering Mechanics, Iowa State University, Ames, 50011, IA, 2002.

[2] Hiramatsu K, Soma H, "*Response Parameters for Characterizing Vehicle Behaviour Under Lateral Wind Disturbance*", C466/009/93, IMechE, 1993.

[3] Yip C K, Crolla D A, Horton D N L, "*The Influence of Aerodynamic Effects on Car Handling*", IMechE 925043, 1992.

[4] Kee J D, Kim M S, Lee J H, "*The aerodynamic Effect on High Speed Stability and Crosswind Stability*", Hyundai Motor Company, Korea, 2003.

[5] Mac Adam C C, "*The Interaction of Aerodynamic Properties and Steering System Characteristics on Passenger Car Handling*", The Dynamics of Vehicle on Road and Tracks (Vehicle System Dynamics-Vol. 18), 11th IAVSD Symposium, 1989.

[6] Milliken W F, Milliken D L, "*Race Car Vehicle Dynamics*", SAE International, Warrendale, 1995.

[7] Russell J B, "*Aerodynamic Effects on the Lateral Control and Stability of Motor Vehicles*", 1st Symposium on Road Vehicle Aerodynamics, The City University, London, Nov 1969.

[8] Scibor-Rylski A J, "*Road Vehicle Aeodynamics*", Pentech Press Limited, London, UK, 1975.

[9] Zhenggi G, Fang G, Jun W, "*Investigation of the Transient State Steering Stability in Side Winds for High-Speed Vehicle*", Int. Journal of Vehicle Design, Vol.26. No.5, 2001.

[10] Goetz H, "*Crosswind Facilities and Procedures*", SAE SP-1109, Warendale 1995.

[11] Howell J P, "*Shape Features which Influence Crosswind Sensitivity*", C466/036/93, IMechE 1993.

[12] Howell J P, "*The Side Load Distribution on a Rover 800 Saloon Car Under Crosswind Conditions*", Journal of Wind Engineering and Industrial Aerodynamics, 60 (1996) 139-153.